IEEE Access
Multidisciplinary | Rapid Review | Open Access Journal

Received February 13, 2021, accepted February 24, 2021, date of publication March 9, 2021, date of current version March 18, 2021.

Digital Object Identifier 10.1109/ACCESS.2021.3064812

A Frequency-Domain Tuning Method for a Class of Reset Control Systems

ALI AHMADI DASTJERDI, (Member, IEEE), AND S. HASSAN HOSSEINNIA, (Senior Member, IEEE)
Department of Precision and Microsystems Engineering, Delft University of Technology, 2628CD Delft, The Netherlands
Corresponding author: S. Hassan Hosseinnia (s.h.hosseinniakani@tudelft.nl)

This work was supported by the NWO, through OTP TTW Project, under Grant 16335.

ABSTRACT Constant in gain Lead in phase (CgLp) compensators, which are a type of reset elements, have shown high potential to overcome limitations of linear control systems. There are few works which investigate the tuning of these compensators. However, there are some significant drawbacks which make those methods unreliable. First, their analyses are performed in the open-loop configuration which do not guarantee the existence of steady-state response of the closed-loop. If it is guaranteed, unlike linear control systems, open-loop analyses cannot precisely predict the closed-loop steady-state performance. In addition, the stability condition could not be assessed during the tuning process. These significant challenges have been separately solved in our recent works by proposing frequency-domain frameworks for analyzing the closed-loop performance and stability of reset control systems. However, they are not formulated and implemented for tuning CgLp compensators. In this paper, based on the loop-shaping approach, the recent frequency-domain framework and the frequency-domain stability method are utilized to provide a reliable frequency-domain tuning method for CgLp compensators. Finally, different performance metrics of a CgLp compensator, tuned by the proposed method, are compared with those of a PID controller on a precision positioning stage. The results show that this method is effective, and the tuned CgLp can achieve more favorable dynamic performance than the PID controller.

INDEX TERMS Reset controllers, constant in gain lead in phase compensators, pseudo-sensitivities, frequency-domain tuning method, loop-shaping.

I. INTRODUCTION

Proportional Integral Derivative (PID) controllers have been used in the industry for several decades. However, since they suffer from a fundamental limitation ''water-bed'' effect, satisfying the ever-increasing demands for high precision and accuracy operations calls for a better alternative [1]–[3]. Advanced feedforward control techniques like iterative learning control [4], [5] and non-linear control techniques such as sliding mode control, observer based adaptive control, backstepping control were investigated to improve the performance of motion systems [6]–[9]. Among non-linear controllers, it has been widely demonstrated that reset controllers have prospects to reduce the limitation of linear control systems and got a lot of attention from academia due to their simple structure [10]–[22].

The associate editor coordinating the review of this manuscript and approving it for publication was Zhong Wu.

The first reset element, which is Clegg Integrator (CI), was introduced by Clegg in 1958 [13]. CI is an integrator which resets its state to zero when its input crosses zero. Next, to have more design freedom and applicability, First Order Reset Element (FORE) [10], [23], [24] and Second Order Reset Element (SORE) have been proposed [17], [23]. Furthermore, Fractional Order Conditional Integrator (FOCI), which has the capability of tuning high order harmonics, has been introduced in [25]. Besides, to enhance the performance of reset control systems, several techniques such as reset band [26], [27], fixed reset instants [28], Partial Reset, and PI+CI approaches [29] have been studied.

Considering only the first harmonic of the steady-state output of reset elements (Describing Function (DF) analysis [30]) reveals that reset elements provide less lag phase in comparison with their base linear structures. Based on this phase advantage, several new phase compensators have been proposed [11], [23], [31]–[33]. One of these novel reset compensators is 'Constant in gain Lead in phase' (CgLp) which

has a constant gain with a phase lead [11], [23], [32]. As the consequence of replacing derivative in PID with CgLp [23], [32], the open-loop of the system gets higher gains at low frequencies and lower gains at high frequencies which leads to enhance the closed-loop performance of the system.

There are few studies which investigate tuning of CgLp compensators [23], [32], [34], [35]. In those studies, CgLp compensators are mainly tuned to achieve a specific amount of phase lead at the cross-over frequency considering the DF method. In addition, Higher Order Sinusoidal Input Describing Function (HOSIDF) method is used in some of those methods to increase the accuracy of their approaches. However, these methods have several significant drawbacks which make them unreliable. First and foremost, the condition for the existence of the steady-state performance of the closed-loop, which is essential for relying on the closed-loop performance prediction, has not been checked. Second, the DF method cannot precisely predict the closed-loop performance even considering the open-loop high order harmonics of reset control systems [36]–[45], which results in the differences between the obtained results and the expected performance. Finally, stability could only be assessed after the tuning process. Hence, obtaining a reliable frequency-domain tuning method for CgLp compensators that handles these challenges is still an important open question.

Recently, the sufficient condition for the existence of the steady-state response of the closed-loop reset control systems has been given in [40]. Also, in that work, pseudo-sensitivities for reset control systems are defined which combine high order harmonics to precisely predict the closed-loop steady-state performance of these systems. Furthermore, a frequency-domain method for assessing the stability of reset control systems has been proposed which allows determining the stability during the tuning process [46].

The contributions of this paper to tune CgLp compensators are:

- Based on the loop-shaping approach, we utilize the pseudo-sensitivities [40] and the frequency-domain stability method [46] to provide a reliable frequency-domain tuning method for CgLp compensators.
- To show the effectiveness of the proposed tuning method, a CgLp compensator is tuned and implemented on a high-tech precision positioning stage. Furthermore, the paper delves deeper into the precision position stage performance metrics, like disturbance rejection, noise rejection, tracking performance, obtained using the CgLp compensator.
- Although it is not proven theoretically, we practically show that ''water-bed'' effect is beaten for this application.

Actually, CgLp compensators, which are designed with the proposed method, have a stable steady-state solution, and initial conditions do not affect their performances. Besides, since CgLp compensators are tuned on the basis of pseudo-sensitivities, their performance can be precisely predicted.

In the remainder of this paper, an overview of CgLp compensators is presented in Section II. In Section III, the frequency-domain tuning procedure is elaborated. In Section IV, the tuned CgLp is applied to the precision positioning stage, and its performance is compared with a PID controller. Conclusions are provided in Section V.

II. OVERVIEW OF CGLP COMPENSATORS

In this section, frequency-domain descriptions of reset elements, CgLp compensators, the H_β condition, pseudo-sensitivities, and effects of the filters sequence of reset control systems on the performance of systems are briefly recalled.

A. FREQUENCY-DOMAIN DESCRIPTIONS FOR RESET ELEMENTS

The state-space representation of reset elements is,

$$\begin{cases} \dot{x}_r(t) = A_r x_r(t) + B_r e(t), & e(t) \neq 0, \\ x_r(t^+) = A_\rho x(t), & e(t) = 0, \\ u_r(t) = C_r x(t) + D_r r(t), \end{cases} \tag{1}$$

where A_r, B_r, C_r, and D_r are the dynamic matrices of the base linear system of the reset element, $e(t)$ and $u(t)$ are the input and control input, respectively. States' values after reset action are determined by the resetting matrix A_ρ. In the case of Generalized First Order Reset Element (GFORE), $A_\rho = \gamma$ while in the case of Generalized Second Order Reset Element (GSORE), $A_\rho = \gamma I$, with $-1 < \gamma < 1$ [23]. Note that the transfer function $C_r(sI - A_r)^{-1}B_r + D_r$ is called the base linear transfer function of the reset element.

Similar to other non-linear controllers, the DF analysis is popularly used in literature to study frequency-domain behavior of reset elements. To have a well-defined steady-state response for a sinusoidal reference input $r(t) = a_0 \sin(\omega t)$, it is assumed that A_r has all eigenvalues with a negative real part, and A_ρ has all eigenvalues with a magnitude smaller than one [12]. The sinusoidal input DF of reset elements (1) is given in [12] as

$$\mathcal{N}_r(j\omega) = C_r \left(j\omega I - A_r\right)^{-1} B_r \left(I + j\Theta(\omega)\right) + D_r, \tag{2}$$

in which Θ is

$$\Theta(\omega) = \frac{-2\omega^2}{\pi}(I + e^{\frac{\pi A_r}{\omega}})\Big((I + A_\rho e^{\frac{\pi A_r}{\omega}})^{-1}A_\rho(I + e^{\frac{\pi A_r}{\omega}}) - I\Big)(\omega^2 I + A_r^2)^{-1}. \tag{3}$$

In [36], the DF method is extended to HOSIDF method in which a non-linear controller is considered as a virtual harmonic generator, and HOSIDF is defined as

$$H_n(j\omega) = \frac{a_n(\omega)e^{j\varphi_n(a_0,\omega)}}{a_0}, \tag{4}$$

where a_n and φ_n are the n^{th} component of the Fourier series expansion of the steady-state output of the controller for a

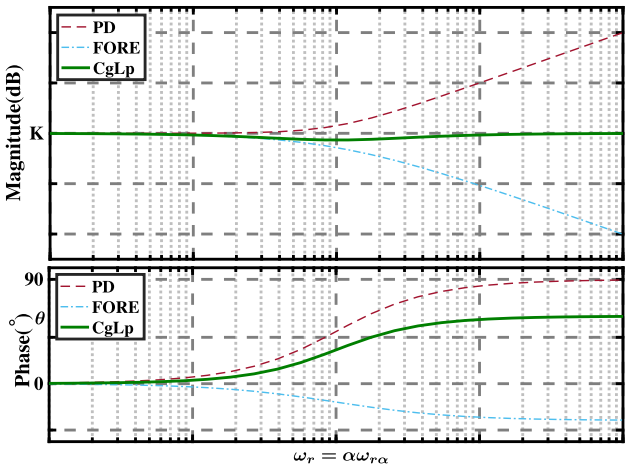

FIGURE 1. The DF of a CgLp compensator when $\omega_t = \infty$.

sinusoidal input. HOSIDF of reset elements in the open-loop configuration is provided in [39] as $H_n(j\omega)$ which is

$$\begin{cases} C_r(j\omega I - A_r)^{-1}(I + j\Theta(\omega))B_r + D_r, & n = 1, \\ C_r(jn\omega I - A_r)^{-1} j\Theta(\omega)B_r, & n > 1 \text{ odd}, \\ 0, & n \text{ even}, \end{cases} \tag{5}$$

where n is the order of harmonics.

B. CGLP COMPENSATOR

A CgLp compensator (6) is constructed utilizing a GFORE or a GSORE with the series combination of a corresponding order of a lead filter. Considering the DF analysis, at the frequency range of ω_r till ω_t, the controller shows a constant gain with a phase lead, as the gain slope of GFORE will cancel the gain slope of the lead filter (Fig. 1) [11], [23], [47]. In this paper, without loss of generality, we consider the first order CgLp which is

$$C_{CgLp}(s) = \left(\frac{1}{\frac{s}{\omega_{r\alpha}} + 1}\right)^{A_\rho} \left(\frac{\frac{s}{\omega_r} + 1}{\frac{s}{\omega_t} + 1}\right), \tag{6}$$

where $\omega_{r\alpha}$ is the corner frequency of the reset element, $A_\rho = \gamma$ is the reset matrix ($(\nearrow)^{A_\rho}$ denotes the controller resets with the reset matrix A_ρ), and ω_d and ω_t are the corner frequency of the lead filter. To provide a constant gain, $\omega_{r\alpha} = \omega_r/\alpha$, where α is a correction factor which is provided in Table 1, and $\omega_t \gg \omega_r$. Since the CgLp compensator has a constant gain with a positive phase, the stability margin will increase while it does not amplify the sensitivity of the system to noise considering the DF method.

C. H_β CONDITION

There exist several approaches to determine the stability of reset control systems [14], [29], [48]–[50]. Among these methods, the H_β condition method [29], [48] received a lot of attention due to its simplicity and frequency-domain applicability. In [46], a method is proposed to test the H_β condition using the frequency response of the plant directly. Let $L(j\omega)$ and $C_R(j\omega)$ be the frequency response of the base linear of the open-loop and of the reset element, respectively. Then, the Nyquist Stability Vector (NSV$= \vec{\mathcal{N}}(\omega) \in \mathbb{R}^2$), for all $\omega \in \mathbb{R}^+$, is $\vec{\mathcal{N}}(\omega) = [\mathcal{N}_\chi \quad \mathcal{N}_\Upsilon]^T$ in which

$$\mathcal{N}_\chi = \left|L(j\omega) + \frac{1}{2}\right|^2 - \frac{1}{4},$$
$$\mathcal{N}_\Upsilon = \Re(L(j\omega) \cdot C_R(j\omega)) + \Re(C_R(j\omega)).$$

Now, considering $\theta_1 = \min_{\omega\in\mathbb{R}^+} \angle\vec{\mathcal{N}}(\omega)$ and $\theta_2 = \max_{\omega\in\mathbb{R}^+} \angle\vec{\mathcal{N}}(\omega)$, the H_β condition can be examined by the following theorem [46].

Theorem 1: Suppose $-1 < \gamma \leq 1$. Then, the H_β condition for a reset control system is satisfied and its response is uniformly bounded-input bounded-state (UBIBS) stable if

$$\left(-\frac{\pi}{2} < \theta_1 < \pi\right) \wedge \left(-\frac{\pi}{2} < \theta_2 < \pi\right) \wedge (\theta_2 - \theta_1 < \pi). \tag{7}$$

D. PSEUDO-SENSITIVITIES FOR RESET CONTROL SYSTEMS

For Linear Time Invariant (LTI) systems, the tracking error and required control action are calculated by sensitivity transfer functions. Although reset control systems may be analyzed using the DF method in the closed-loop, this yields an approximation which is not precise due to the existence of high order harmonics. In order to analyze reset control systems more accurately, pseudo-sensitivity functions for a sinusoidal reference $r(t) = r_0 \sin(\omega t)$ are defined in [40] to combine all high order harmonics to a single function. To this end, the sufficient condition for the existence of the steady-state solution is asserted in [40].

Theorem 2: A closed-loop reset control system has a well-defined steady-state solution for any Bohl function input if the H_β condition is satisfied and reset instants have the well-posedness property [40].

Also, the tracking error and control input of a reset control system for $r(t) = \sin(\omega t)$ is a periodic function with the period of $2\pi/\omega$ if the H_β condition is satisfied. Therefore, from the precision viewpoint, the pseudo-sensitivity can be defined as the ratio of the maximum error of the reset control system with $r(t) = r_0 \sin(\omega t)$ to the amplitude of the reference at each frequency.

Definition 1: Pseudo-sensitivity S_∞

$$\forall\omega \in \mathbb{R}^+ : \; S_\infty(j\omega) = e_{\max}(\omega)e^{j\varphi_{max}},$$

where

$$e_{\max}(\omega) = \left(\frac{\max\limits_{t_{ss_0} \leq t \leq t_{ss_m}} (r(t) - y(t))}{r_0}\right)$$
$$= \sin(\omega t_{\max}) - \frac{y(t_{\max})}{r_0},$$

TABLE 1. Correction factor α of first order CgLp [23].

γ	-0.9	-0.8	-0.7	-0.6	-0.5	-0.4	-0.3	-0.2	-0.1	0	0.1	0.2	0.3	0.4	0.5	0.6	0.7	0.8	0.9
α	16.71	8.19	5.26	3.85	3.01	2.47	2.09	1.81	1.60	1.44	1.32	1.23	1.16	1.11	1.07	1.04	1.02	1.01	1.0

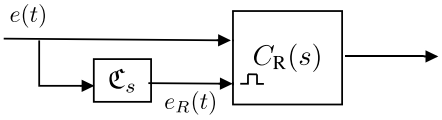

FIGURE 2. Structure of the shaping filter.

$\varphi_{max} = \frac{\pi}{2} - \omega t_{max}$, $y(t)$ is the response of the closed-loop reset control system, and t_{ss_0} and $t_{ss_m} = t_{ss_0} + \frac{2\pi}{\omega}$ are the steady-state reset instants of the closed-loop reset control system ($e(t_{ss_0}) = e(t_{ss_m}) = 0$). Similarly, pseudo-control sensitivity $CS_\infty(j\omega)$ (frequency response from reference to control input), pseudo-complementary sensitivity $T_\infty(j\omega)$ (frequency response from reference to the output of the system), and pseudo-process sensitivity $PS_\infty(j\omega)$ (frequency response from disturbance to the error of the system) are defined in [40].

E. SEQUENCE OF RESET ELEMENTS

Unlike linear controllers, the sequence of filters of reset control systems affects the performance of these systems, which is investigated in [44]. It is revealed that if the sequence of the control parts is lead elements of the linear controller, reset element, and lag elements of the linear controller, then, the system has a better tracking performance in some frequencies than other sequences. Also, using this sequence, the reset control system has an over-damp step response, and its rise time is increased (also seen in [51]). However, the performance of the system is drastically hampered in this sequence if the signal to noise ratio is low. To solve this issue, a shaping filter $\mathfrak{C}_s$ is used to roll-off the noise from the reset instants of the reset control system as shown in Fig. 2. The transfer function of the shaping filter is described in [44] as

$$\mathfrak{C}_s = \left(\frac{1}{1+\frac{s}{2\omega_c}}\right)\left(\frac{1+\frac{1.62s}{\omega_c}}{1+\frac{s}{1.62\omega_c}}\right), \tag{8}$$

in which ω_c is the cross-over frequency of the open-loop considering the DF method. In this research, we use the traditional configuration, in which the tracking error is the input of the reset element. Also, we will analyze the performance of different sequences of filters of a reset control system experimentally.

III. TUNING PROCEDURE

In this section, the pseudo-sensitivities and the frequency-domain stability method are utilized based on the loop-shaping approach [52]–[59] to provide an appropriate frequency-domain tuning method for CgLp compensators.

The structure of the controller C_R is CgLp.PID as

$$C_R = \overbrace{K_p \underbrace{\overbrace{\left(\frac{1}{\frac{\alpha s}{\omega_r}+1}\right)^{\gamma}}^{\text{FORE}}\overbrace{\left(\frac{\frac{s}{\omega_r}+1}{\frac{s}{\omega_t}+1}\right)}^{\text{Lead}_1}}_{\text{CgLp}}\overbrace{\left(1+\frac{\omega_i}{s}\right)}^{\text{PI}}\overbrace{\left(\frac{\frac{s}{\omega_d}+1}{\frac{s}{\omega_f}+1}\right)}^{\text{Lead}_2}}^{\text{PID}}, \tag{9}$$

in which set (K_p, ω_r, γ, ω_d, ω_t, ω_f, ω_i) is the tuning parameter set, and α is provided in Table 1. Following the loop-shaping method described in [52], to have an acceptable rise time, control effort level, tracking performance, and disturbance and noise rejection capabilities, four frequency-domain inequality constraints (Fig. 3)

$$|T_\infty(j\omega)| \leq |T_u(\omega)|, \tag{10}$$
$$|S_\infty(j\omega)| \leq |S_u(\omega)|, \tag{11}$$
$$|CS_\infty(j\omega)| \leq |CS_u(\omega)|, \tag{12}$$
$$|PS_\infty(j\omega)| \leq |PS_u(\omega)|, \tag{13}$$

have to be fulfilled, for all $\omega \in \mathbb{R}^+$. As shown in Fig. 3a, $S_u(j\omega)$ restrains the lowest value of the cross-over frequency, limits the magnitude of the peak of sensitivity, and guarantees an acceptable tracking performance. $T_u(j\omega)$ (Fig. 3b) limits the effect of noise on the performance of the system. Moreover, $PS_u(j\omega)$ (Fig. 3c) places a limit on the effects of the disturbance on the system performance, and $CS_u(j\omega)$ (Fig. 3d) confines the control effort level. Besides, to assure stability and be allowed to use pseudo-sensitivities, the tuning parameter set has to satisfy the conditions of Theorem 1. Furthermore, to make the controller robust against gain variations (iso-damping), the tuning parameter set is selected such that

$$\frac{d(\angle \mathcal{N}_{CgLp}(j\omega)\text{PID}(j\omega)G(j\omega))}{d\omega}\Big|_{\omega=\omega_c} = 0, \tag{14}$$

in which

$$\mathcal{N}_{CgLp}(j\omega) = \mathcal{N}_r(j\omega)\left(\frac{\frac{j\omega}{\omega_r}+1}{\frac{j\omega}{\omega_t}+1}\right), \tag{15}$$

and ω_c is obtained by

$$|\mathcal{N}_{CgLp}(j\omega_c)\text{PID}(j\omega_c)G(j\omega_c)| = 1. \tag{16}$$

All in all, the considered constraints for tuning the control structure (9) are summarized as:

(I) The H_β condition: Equation (7) and $-1 < \gamma \leq 1$
(II) Iso-damping behaviour: Equation (14)

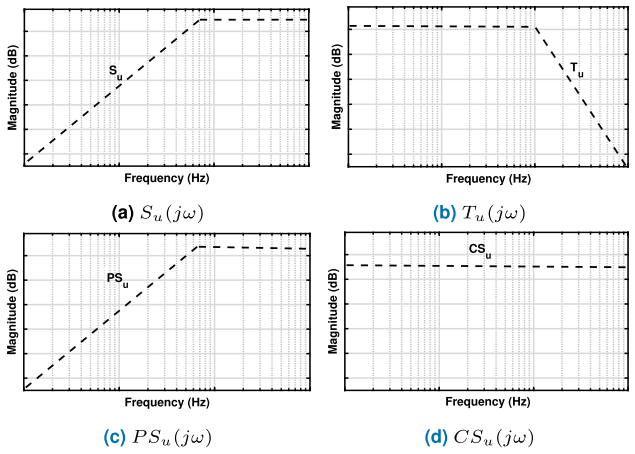

(a) $S_u(j\omega)$ (b) $T_u(j\omega)$ (c) $PS_u(j\omega)$ (d) $CS_u(j\omega)$

FIGURE 3. Loop-shaping constraints.

(III) Loop-shaping constraints: Equations (10)-(13)

Now, it is needed to define a suitable cost function to accomplish the tuning procedure of the control structure (9). According to [52], to have a more favorable tracking performance in the interested region of frequencies, the following cost function is obtained.

$$J = \max_{\omega \le \omega_l} \left| \frac{S_\infty(j\omega)}{\omega} \right|_{\text{dB}}, \tag{17}$$

where $\omega_l \le \omega_c$ determines the interested region of frequencies over which the reset control system is expected to track references and reject disturbances.

A. SOLVING THE OPTIMIZATION PROBLEM

For simplicity, the control structure (9) is re-written as

$$C_{\text{R}}(s) = K_p \overbrace{\underbrace{\left(\frac{1}{\frac{\alpha\chi_1}{\omega_c}s + 1}\right)^{\gamma}}_{\text{FORE}} \underbrace{\left(\frac{\frac{\chi_1}{\omega_c}s + 1}{\frac{1}{\chi_2\omega_c}s + 1}\right)}_{\text{Lead}_1}}^{\text{CgLp}} \times \overbrace{\underbrace{\left(1 + \frac{\omega_c}{\chi_3 s}\right)}_{\text{PI}} \underbrace{\left(\frac{\frac{\chi_4}{\omega_c}s + 1}{\frac{1}{\chi_5\omega_c}s + 1}\right)}_{\text{Lead}_2}}^{\text{PID}}, \tag{18}$$

in which $\chi_i > 0$ and $-1 < \gamma \le 1$. In addition, limits for ω_c is found based on $S_u(j\omega)$ and $T_u(j\omega)$. Here, we use Genetic Algorithm (GA) method for solving this optimization problem. To speed up the process, we propose the following procedure:

- For each potential solution $(\omega_c, \gamma, \chi_1, \chi_2, \chi_3, \chi_4, \chi_5)$ produced by the GA method, α and K_p are obtained by γ (Table 1) and (16), respectively.
- Check constraint (I), (II), and (III) in tandem to reduce computational efforts.
- If all constraints are satisfied, calculate J (18).
- Continue until the stop criterion of the GA method are satisfied.

1) PROVIDE AN APPROPRIATE INITIAL GUESS

Here, we provide a method to obtain an appropriate initial guess for the GA method. To this end, we suggest using a grid search method to explore an appropriate feasible solution. First, provide a wide range for χ_i considering $S_u(j\omega)$, $T_u(j\omega)$, $PS_u(j\omega)$, and stability of the base linear of the system. Suppose we obtain vectors l_B and u_B which set the lower and higher limits for the tuning parameter set (i.e. $l_B < [\omega_c\ \gamma\ \chi_1\ \chi_2\ \chi_3\ \chi_4\ \chi_5]^T < u_B$). Then, with a small resolution, we grid the parameters and provide a parameter space. Now, we check constraints (I)-(III) in tandem for every point in this space and eliminate the points which do not satisfy the constraints. Finally, suppose there are N parameter sets which satisfy the aforementioned constraints, then the parameter set with the minimum J value is selected as the initial guess for the optimization problem proposed in Section III-A. Since the performance of the controller is not so sensitive to a small change of the tuning parameter set, it is highly possible that this initial guess does not have a far distance from the final solution of the GA method.

IV. APPLICATION TO A PRECISION MOTION STAGE

To show the effectiveness of the proposed tuning method, a precision positioning stage (Fig. 4), which is termed "Spider", is considered as a benchmark. In this system, three actuators are angularly spaced to actuate three masses (labeled by B1, B2, and B3) which are constrained by parallel flexures and connected to the central mass D through leaf flexures. Only one of the actuators (A1) is considered and used for controlling the position of mass B1 attached to the same actuator which results in a SISO system. A linear power amplifier is utilized to drive the Lorentz actuator, and Mercury M2000 linear encoder is used to obtain position feedback with a resolution of 0.1 μ m.

The identified frequency response data of the system is shown in Fig. 5.

As illustrated in Fig. 5, although the plant is a collocated double mass-spring system, the identified frequency response data is well approximated by a mass-spring-damper system via the transfer function

$$G(s) \approx \frac{Ke^{-\tau s}}{\frac{s^2}{\omega_r^2} + \frac{2\zeta s}{\omega_r} + 1} = \frac{1.14e^{-0.00014s}}{\frac{s^2}{7627} + \frac{0.05s}{87.3} + 1}. \tag{19}$$

Note that to use relations provided in [40], the time delay ($e^{-0.00014s}$) is approximated by the first order Pade method [60] as $(-s + 14400)/(s + 14400)$. To provide an acceptable closed-loop performance for the positioning stage, without loss of generality, we consider similar constraints as in [52]:

$$T_u(\omega) = \begin{cases} 5\text{ dB}, & \omega \le 200\pi, \\ \left(\frac{850}{\omega}\right)^2, & \omega > 200\pi, \end{cases}$$

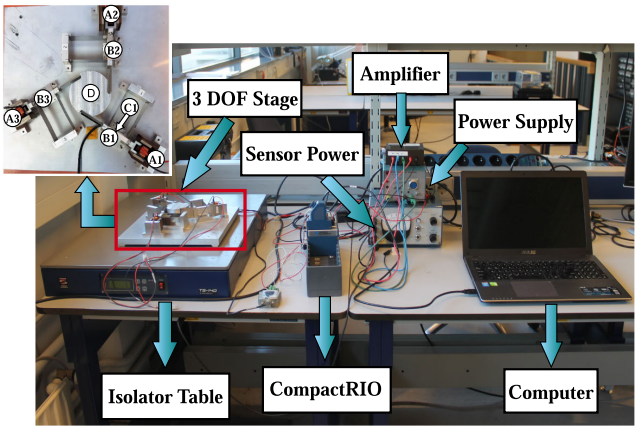

FIGURE 4. The whole setup including computer, CompactRio, power supply, sensor power, amplifier, isolator, sensor and, stage.

$$S_u(\omega) = \begin{cases} \dfrac{\omega}{300}, & \omega \le 160\pi, \\ 4.5\ \text{dB}, & \omega > 160\pi, \end{cases}$$

$$PS_u(\omega) = \begin{cases} \dfrac{\omega}{600}, & \omega \le 30\pi, \\ -15\ \text{dB}, & \omega > 30\pi, \end{cases} \quad \text{and} \quad CS_u(\omega) = 60\ \text{dB}.$$

Figure 6 shows the frequency behavior of T_u, S_u, PS_u, and CS_u. Since the cut-off frequency of T_u and S_u are 150 Hz and 50 Hz, respectively, ω_c is limited to 50 Hz $< \omega_c <$ 150 Hz. Moreover, we take $\omega_l = 20\pi$ as the maximum limit of the interest frequency region for tracking. Now, the control structure (9) is tuned based on the described method in Section III. To simplify constraint (II), according to phase plot of the stage (Fig. 5) and the variation range of ω_c (50 Hz,150 Hz), we can approximate $\left.\frac{d(\angle G(j\omega))}{d\omega}\right|_{\omega=\omega_c} \approx -\tau$. Therefore, constraint (II) can be re-written as

$$\left.\frac{d(\angle \mathcal{N}_{CgLp}(j\omega) + \angle \text{PID}(j\omega))}{d\omega}\right|_{\omega=\omega_c} \approx \tau = 0.00014. \quad (20)$$

To this end, as described in Subsection III-A1, we consider a wide parameter range for tuning parameters as $[100\pi \ -1\ 1\ 2\ 2\ 2\ 2]^T < [\omega_c\ \gamma\ \chi_1\ \chi_2\ \chi_3\ \chi_4\ \chi_5]^T < [300\pi\ 1\ 20\ 20\ 20\ 10\ 20]^T$ to find an appropriate initial guess for the GA method. The initial guess is obtained as $[190\pi\ 0.5\ 2\ 10.8\ 7.5\ 3.4\ 1.7]^T$. Then, the control structure (9) is tuned by the method presented in Subsection III-A. The tuned CgLp.PID controller is:

$$C_{\text{R}} = 17.05 \left(\frac{1}{\frac{s}{86\pi}+1}\right)^{0.3} \left(\frac{\frac{s}{100\pi}+1}{\frac{s}{1440\pi}+1}\right) \times \left(1+\frac{20\pi}{s}\right)\left(\frac{\frac{s}{66\pi}+1}{\frac{s}{300\pi}+1}\right). \quad (21)$$

As predicted before, the optimum point is not so far from the initial guess. This happens because the closed-loop performance is not so sensitive to a small change of the tuning

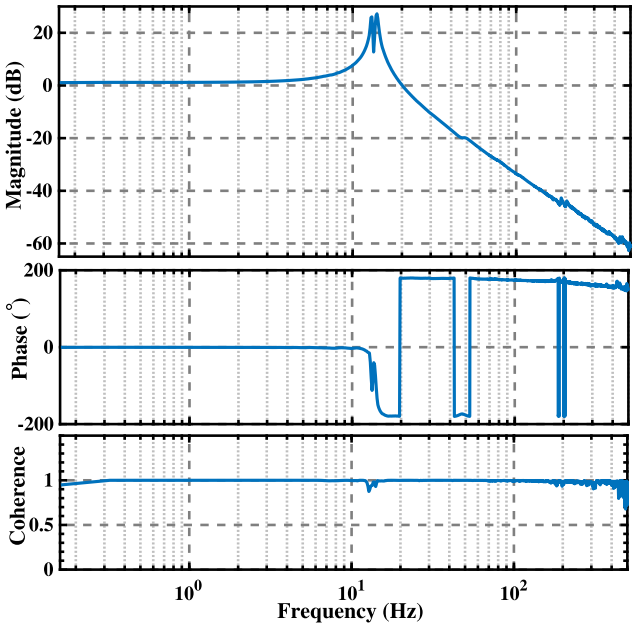

FIGURE 5. Frequency response of the stage.

set parameter which implies that a grid search with a small resolution also can converge to the optimum point. In order to compare the performance of the tuned controller with a linear controller, a PID structure is also tuned with the same method explained in Section III. To have a fair comparison, the structure of the PID controller is similar to the control structure (9) in which FORE is replaced with a low-pass filter. Finally, the C_{PID} is tuned as:

$$C_{\text{PID}} = 7.28 \left(\frac{1}{\frac{s}{1480\pi}+1}\right)\left(\frac{\frac{s}{105\pi}+1}{\frac{s}{360\pi}+1}\right) \times \left(1+\frac{46.5\pi}{s}\right)\left(\frac{\frac{s}{90\pi}+1}{\frac{s}{300\pi}+1}\right). \quad (22)$$

Figure 7 presents the open-loop frequency response of the system with controllers C_{PID} and the DF of the open-loop of the system with the controller C_{R}. As it is observed, the system with the controller C_{R} has a higher cross-over frequency in comparison with the one with the controller C_{PID}. Moreover, the system with these controllers must indicate iso-damping behavior as a result of the flatness region around the cross-over frequency.

The closed-loop frequency responses of the systems with the controller C_{R} including the pseudo-sensitivities and the DF methods, and the closed-loop sensitivities of the system with the controller C_{PID} are also shown in Fig. 6. These frequency responses are obtained utilizing the toolbox in [61]. As illustrated in Fig. 6a, the disturbance rejection capability of the system with the controller C_{R} is better than that of with the controller C_{PID}. Besides, the control input of the system with the controller C_{R} is more than the one with the controller

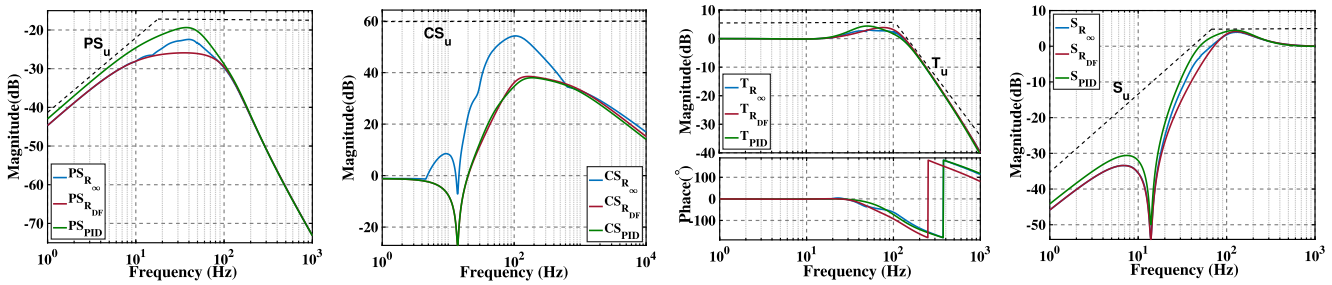

(a) Process sensitivity (b) Control sensitivity (c) Complementary sensitivity (d) Sensitivity

FIGURE 6. The DFs (._ DF) and pseudo-sensitivities (._ ∞) of the closed-loop of the system with the controllers C_R, and the closed-loop sensitivities of the system with the controller C_{PID}.

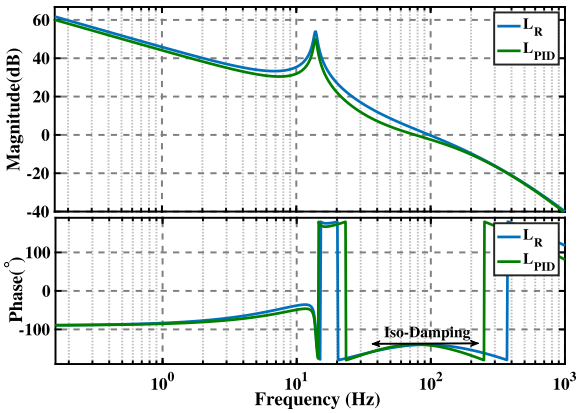

FIGURE 7. Open-loop frequency responses of the system with controllers C_{PID} and C_R.

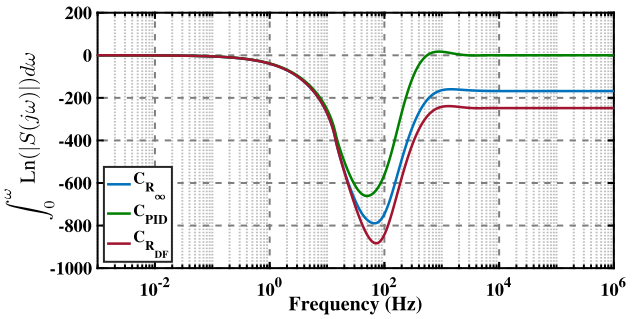

FIGURE 8. The magnitude of the integral of the sensitivity versus frequency.

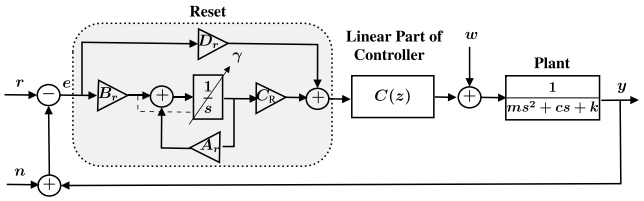

FIGURE 9. The block diagram of the whole system for implementing the designed controllers (reset matrices are discretized).

C_{PID}. This is explained by the fact that reset elements produce jumps in their output signal and differentiation of jumps produces a large control input. Moreover, there are discrepancies between the results obtained by the DF method and pseudo-sensitivities at certain frequency ranges which are due to the existence of high order harmonics. This implies that using pseudo-sensitivities for tuning CgLp compensators is more reliable than using the DF method, particularly for precision motion applications.

As shown in Fig. 6c, the noise rejection capabilities of the system with these two controllers are the same (the same roll-off at high frequencies). Furthermore, as shown in Fig. 6d, the system with the controller C_R has a better tracking performance than that of with the controller C_{PID} at frequencies less than 100Hz while the peak value of the sensitivity of the system with the controller C_R is less than that of with the controller C_{PID}.

A. BREAKING WATER-BED EFFECT

To recall, according to linear control theory,

$$\int_0^\infty \mathrm{Ln}(|S(j\omega)|)d\omega = 0, \tag{23}$$

for every stable Linear Time Invariant (LTI) system which has at least two more poles than zeros. Thus, if the sensitivity amplitude is reduced by some control actions in a certain frequency range, then the sensitivity will increase in other frequency ranges. We calculate this integral numerically for the system with both controllers C_R and C_{PID} (Fig. 8). For the case of C_R, this integral is calculated using the DF method and pseudo-sensitivity. As observed in Fig. 8, the integral (23) for the system with the controller C_{PID} converges to zero as expected by linear control theory. Whereas, the integral (23) for the system with the controller C_R converges to -160 and -250 using the pseudo-sensitivity and the DF method, respectively. This implies that the sensitivity is decreased in a certain frequency range without increasing in other frequency ranges. Note that calculating relation (23) using the DF method is the ideal performance which can be obtained using CgLp compensators. However, using pseudo-sensitivity for calculating this integral for the controller C_R consider all high order harmonics. Although high order harmonics lead to deviation from the ideal case, CgLp compensator is still better than the PID controller and breaks the water-bed effect.

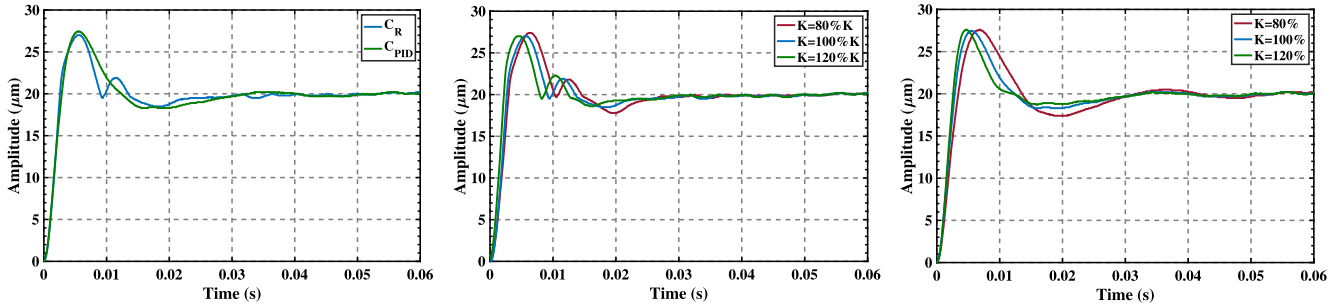

(a) Step responses of controllers **(b)** Iso-damping behavior of C_{R} **(c)** Iso-damping behavior of C_{PID}

FIGURE 10. The step responses of controllers with gain variation between 80% to 120% of their nominal values.

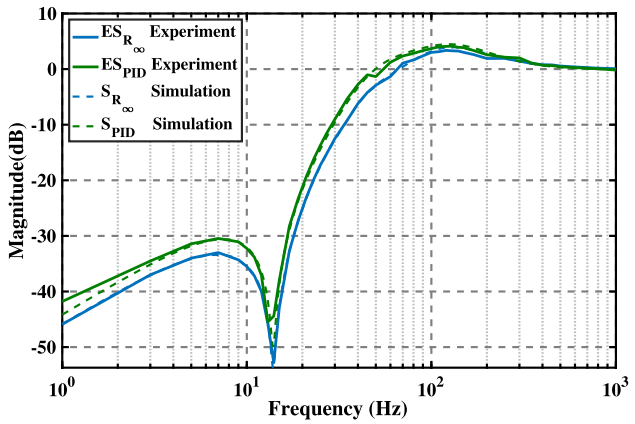

FIGURE 11. The pseudo-sensitivity and sensitivity of the system with the CgLp and PID controllers which are deduced experimentally, ES_{R_∞} and ES_{PID} are practical sensitivity of the system with the controller C_{R} and C_{PID}, respectively.

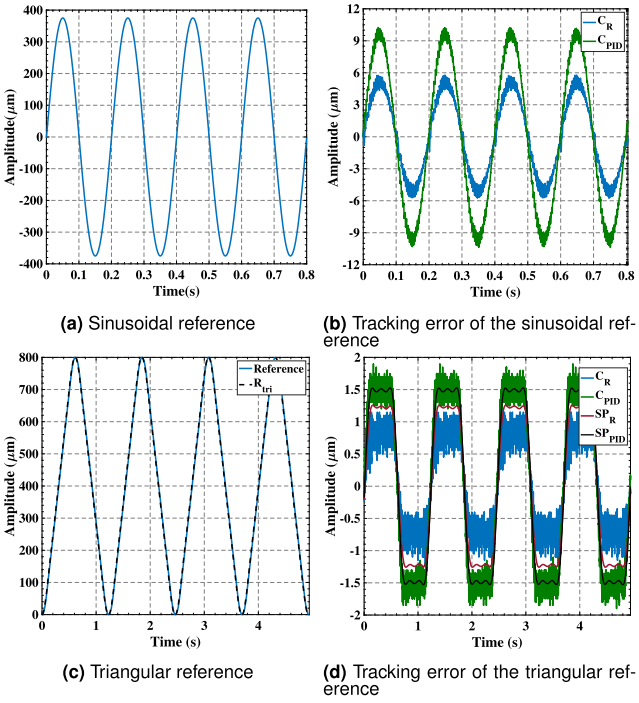

(a) Sinusoidal reference **(b)** Tracking error of the sinusoidal reference

(c) Triangular reference **(d)** Tracking error of the triangular reference

FIGURE 12. Tracking performance of the system with the designed controllers for a triangular and a sinusoidal references. SP_{R} and SP_{PID} are obtained using super-position law and sensitivity responses for three harmonics of R_{tri} which resembles the triangular reference, respectively.

B. TIME-DOMAIN RESULTS

In this part, the time domain results of the system with these two designed controllers are compared with each other. To implement these designed controllers (Fig. 9), each controller is discretized with the sample time $T_s = 100\ \mu$ s using the Tustin method [52], [62]. Furthermore, to provide the well-posedness property (see [29], [48]), we prevent consecutive reset instants.

In Fig. 10, the step responses (step of 20 μ m) of the system with these controllers are shown. The step responses have almost the same rise and settling time while the overshoot of the system with the controller C_{R} is less than that of with the controller C_{PID} as the peak of the sensitivity of the system with the controller C_{R} is less than the one with the controller C_{PID}. To examine the iso-damping behavior of the system, the K_p values of the controllers are changed between 80% to 120% of their nominal values. As it is observed, step responses of these perturbed systems show the same overshoot.

In order to compare the tracking performances of the systems with both controllers, we draw the sensitivity responses practically (Fig. 11). In other words, Fig. 11 shows $(\max e(t))/r_0$ for the sinusoidal reference in several frequencies. As shown in Fig. 11, S_∞ precisely predicts the maximum error of the system with the controller C_{R} for the sinusoidal references. Besides, it shows that the tracking performance of the system with the controller C_{R} is better than the one with the controller C_{PID} for the sinusoidal reference for all frequencies less than 100 Hz. In order to have a closer look, we show the time response of the system with these controllers for a sinusoidal reference (Fig. 12a) at 5 Hz in Fig. 12b. Moreover, a triangular trajectory with an amplitude of 800 μ m (Fig. 12c) is applied to the system. As shown in Fig. 12d, the system with the controller C_{R} also has a better tracking performance than that of with the controller C_{PID} for the triangular reference, which consists of several frequencies. For this trajectory and sinusoidal references, the tracking performance of the system is improved by 60% using the controller C_{R}.

Similarly, the process-sensitivities of the system with these controllers are practically shown in Fig. 13. As was predicted

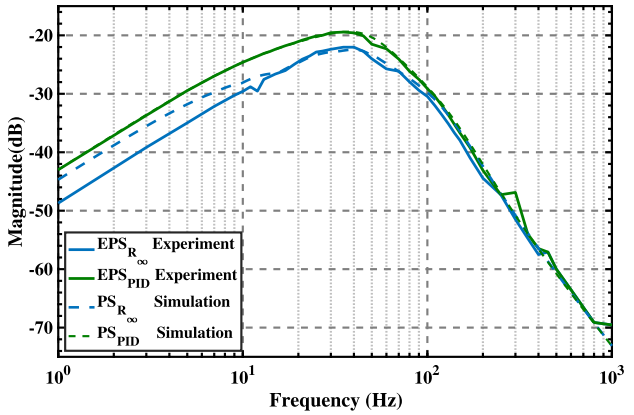

FIGURE 13. The process pseudo-sensitivity and process sensitivity of the system with the CgLp and PID controllers which are deduced experimentally, EPS_{R_∞} and EPS_{PID} are practical process sensitivity of the system with the controller C_R and C_{PID}, respectively.

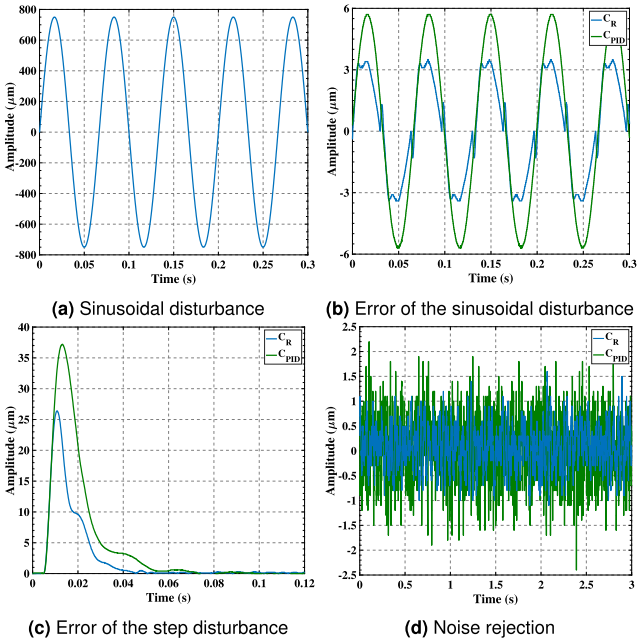

FIGURE 14. Disturbance rejection capability of the system for a step and a sinusoidal disturbance, and noise rejection capability of the system.

in Fig. 6a, the system with the controller C_R has a better disturbance rejection performance than that of with the controller C_{PID} for all frequencies less than 100 Hz. As was seen in Fig. 13, there is a small deviation between pseudo-process sensitivity and the practical results at low frequencies. This deviation is because of quantization and sensor noise of the precision stage, which fortunately reduce effects of disturbances at low frequencies in this case. It can be said that the disturbance rejection capability of the system is enhanced by 70% using the controller C_R for sinusoidal disturbances. To have a closer look, we show the time response of the system with these controllers for a sinusoidal disturbance (Fig. 14a) at 15 Hz in Fig. 14b. Moreover, a step disturbance is applied to the system, and the amplitude of the error is shown in Fig. 14c. As it is shown, the system with the controller C_R attenuates the step disturbance better than that of with

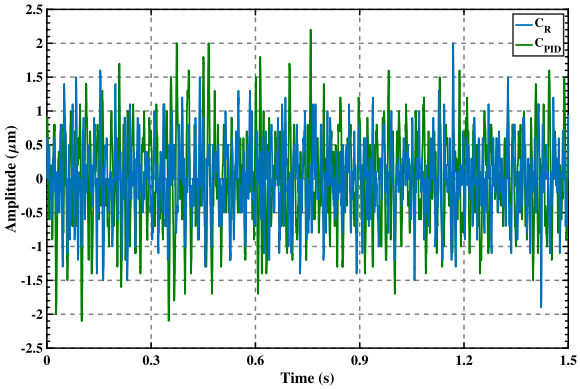

FIGURE 15. Disturbance rejection capability of the system with C_R and C_{PID} for colored noise disturbance.

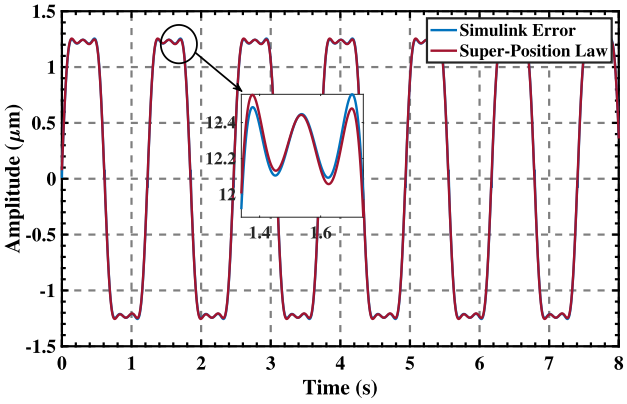

FIGURE 16. Comparison between the predicted error by super-position law and simulated error without quantization and noise for system with C_R.

the controller C_{PID}. In addition, to mimic the floor vibration, a colored noise (white noise multiplied by a band-pass filter), which mainly includes frequencies between 1-30 Hz, is applied to the system and the amplitude of the error is shown in Fig. 15. It is observed that the system with the control C_R also attenuates this disturbance slightly better than the one with the controller C_{PID}. To study the noise rejection capabilities of the system with these controllers, white noise with a maximum amplitude of 5 μ m is applied to the system. Although it was predicted by Fig. 6c that the system with these controllers have the same noise rejection capability, the noise rejection capability of the system with the controller C_R is slightly better than the one with the controller C_{PID} (Fig. 10b).

To sum up, the system with the tuned CgLp compensator has a smaller overshoot, the same rise time, better tracking performance and disturbance rejection capability for frequencies less than 100 Hz, a smaller peak of the sensitivity, and a better noise rejection capability than those of the system with the controller PID.

C. INVESTIGATION OF SUPER-POSITION LAW

In this section, we assess the acceptability of super-position law for the system with the controller C_R. To this end, we consider the triangular trajectory (Fig. 12c), which is the

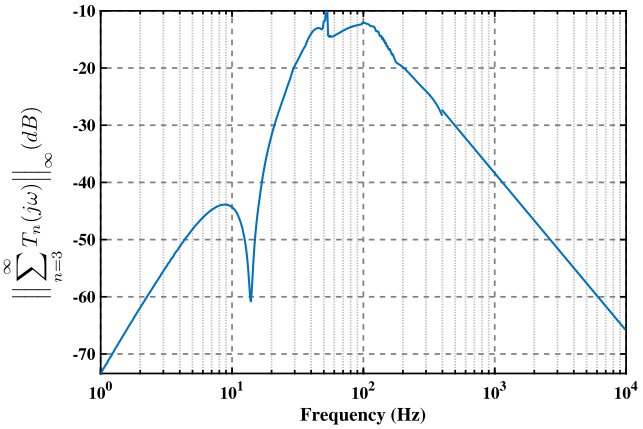

FIGURE 17. The infinity norm of summation of high order harmonics of the complementary-sensitivity of system with the controller C_R.

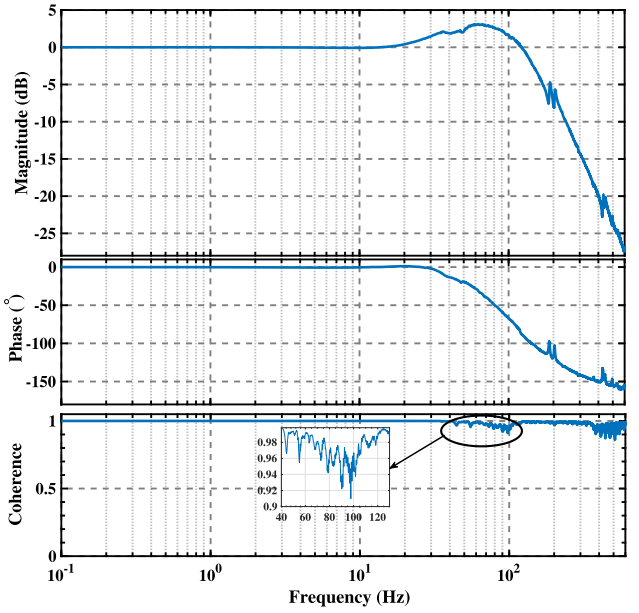

FIGURE 18. Identification of the closed-loop of the system with controller C_R.

combination of several harmonics. As it is shown in Fig. 12c, the reference can be accurately approximated with

$$R_{\text{tri}}(t) = 363.7\sin(5.1t - 1.54) + 31.27\sin(15.3t - 1.5) + 6\sin(25.5t - 1.45) + 400. \quad (24)$$

Since the H_β condition is satisfied and controller C_R has a PI, the steady-state error of tracking is independent of the constant value [14]. In Fig. 12d, the predicted errors, which are obtained using super-position law and sensitivity responses for these three harmonics, for both controllers C_R (SP_R) and C_{PID} (SP_{PID}) are drawn. As it is observed, there are differences (16% maximum relative error) between predicted errors by super-position law and practical errors for both controllers C_R and C_{PID}. These differences are mainly due to quantization and noise of sensor (for more details about effects of noise and quantization on the performance of reset control systems, see [63]). Fortunately, in this application,

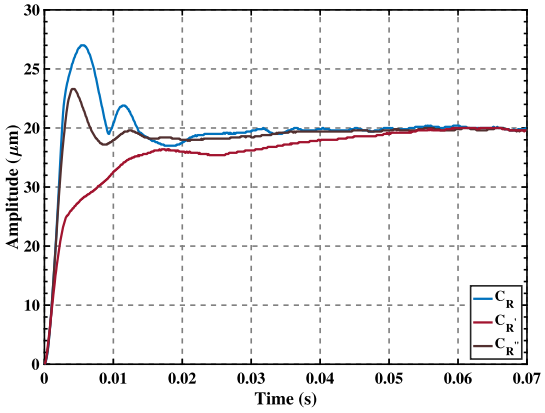

FIGURE 19. Step responses of the system with CgLp compensators.

noise and quantization positively affect the performance and reduce the tracking error. In Fig. 16, we compare the simulation error, in which we do not consider the noise and quantization, and the predicted error obtained by super-position law for controller C_R. As it is seen, when noise and quantization do not exist, the total error almost follows the super-position law for this trajectory.

The identification of the closed-loop system with the controller C_R is demonstrated in Fig. 18. The coherence plot is an indicator of existed noise and non-linearity in the output of the closed-loop system in the presence of the input signal $r(t)$. Since the coherence is almost one at low and high frequencies ($f < 40$ and $f > 120$), the relation between $r(t)$ and $y(t)$ can be precisely approximated as a linear system in this rage of frequency, and we can rely on the super-position law for estimating the tracking error. This can be justified by the fact that in the frequency range ($40 < f < 120$), the high order harmonics amplitudes of the complementary-sensitivity are maximum near the cross-over frequencies, and they are filtered out outside of this frequency range (Fig. 17). In this figure,

$$\left\|\sum_{n=3}^{\infty} T_n(j\omega)\right\|_\infty : \sup_{t_{ss_0}\le t\le t_{ss_m}} \sum_{n=3}^{\infty} |T_n(j\omega)|\sin(n\omega t + \angle T_n(j\omega)),$$

for all $\omega \in \mathbb{R}^+$, which is an appropriate indicator of effects of high order harmonics on the output of the systems (for more details about $T_n(j\omega)$, see [40]). Indeed, there is a relation between the amplitudes of high order harmonics of the complementary-sensitivity and the coherence of identification which should be investigated in a future study.

D. CHANGING SEQUENCE OF RESET ELEMENT

In this subsection, we investigate effects of changing the sequence of control filters C_R on the performance of the precision positioning stage. The controller C_R has the traditional sequence which is FORE-Lead-PI (for the sake of simplicity, Lead means $\text{Lead}_1.\text{Lead}_2$ in (18)). Let's assume C_R, $C_{R'}$, and $C_{R''}$ have the same base linear. The sequence of filters in controllers $C_{R'}$ and $C_{R''}$ is Lead-FORE-PI. In addition, $C_{R''}$ has a shaping filter in the reset-instants line as explained in

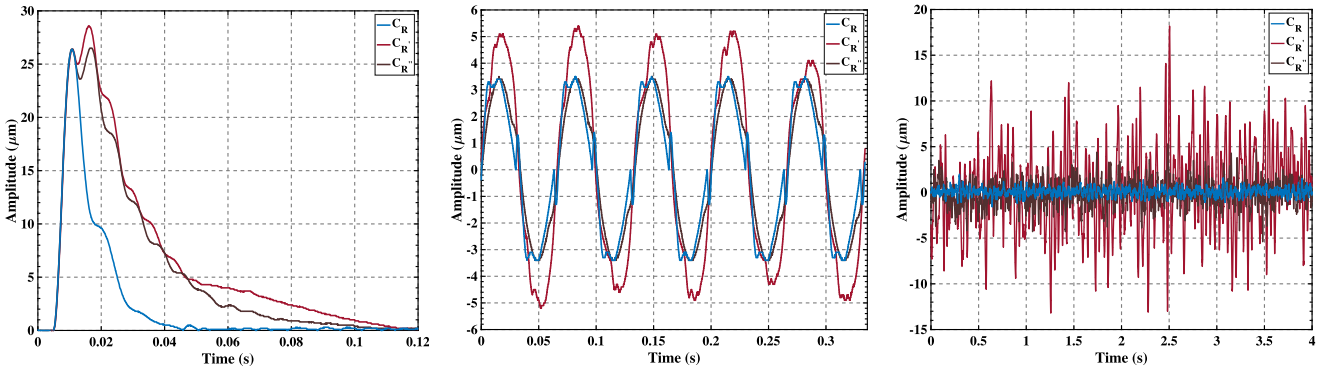

(a) Error of the step diturbance **(b)** Error of the sinusoidal disturbance **(c)** Noise rejection capability

FIGURE 20. Disturbance and noise rejection capability of the system with CgLp controllers.

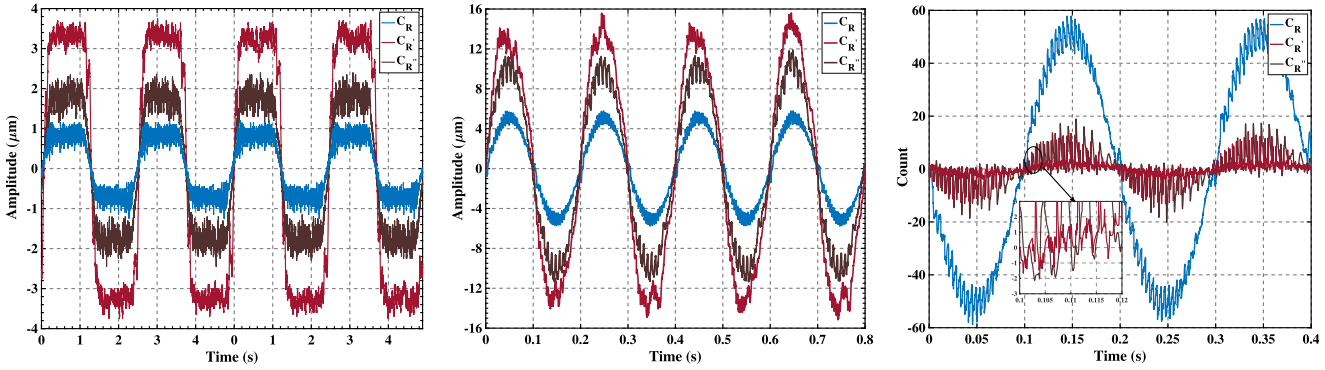

(a) Error of the triangular reference **(b)** Error of the sinusoidal reference **(c)** The input of the reset instant line of the reset element of CgLp controllers

FIGURE 21. Tracking performance of the system with CgLp controllers and the input of the reset instant line.

Subsection II-E. Note that since changing sequence does not alter the H_β condition [64], the H_β condition is also satisfied for the system with the controller $C_{R'}$, and the stability of the system with the controller $C_{R''}$ is assured with the method described in [64].

In Fig. 19, the step responses (step of 20 μ m) of the system with these CgLp controllers are shown. As it is shown, the system with the controller $C_{R''}$ has less over-shoot than that of with the controller C_R. Furthermore, the system with the controller $C_{R'}$ has an over-damp response with the highest rise and settling time. It can be said that this configuration is similar to a reset system which resets when the differentiation of the tracking error is zero ($\dot{e}(t) = 0$). Consequently, the reset control system resets sooner than the case in which the resetting law is $e(t) = 0$. This can be the reason for the over-damp response with high settling time. It is noteworthy to recall that the open-loop DFs of the system with controllers C_R and $C_{R'}$ are exactly the same. However, the step response specifications, including rise time and over-shoot, are totally different due to different amplitudes of high order harmonics. Thus, the effect of the structure of reset elements on the accuracy of the DF method can be considered as an interesting topic for a future study.

The disturbance rejection capabilities of the system with these CgLp controllers for the step disturbance and the sinusoidal disturbance at 15 Hz are shown in Fig. 20a and Fig. 20b, respectively. Besides, a white noise with a maximum amplitude of 5 μ m is applied to examine the noise rejection capabilities of the system with these CgLp controllers (Fig. 20c). The system with controller C_R has the best disturbance and noise rejection capabilities among these CgLp controllers. Similarly, using the shaping filter significantly improves the disturbance and noise rejection capabilities of the system with controller $C_{R'}$.

To see effects of changing sequence on the tracking performance, the triangular reference and the sinusoidal reference at 5 Hz are applied to the system (Fig. 21). As shown in Fig. 21a and Fig. 21b, the system with the controller C_R has the best tracking performance for the triangular and the sinusoidal references. As discussed in [44], for low frequency references, when the lead element of the controller comes first, the existed noise and quantization error are amplified and dominate the tracking error. Consequently, the reset instants are considerably changed by amplified noise which deteriorates the tracking performance of the system. In this case, as suggested in [44], using the shaping filter ($C_{R''}$) solves the problem to some extend. To show this, in Fig. 21c, we illustrate the signal that enters the reset line of the reset element for these CgLp controllers as a result of the sinusoidal input at 5 Hz in the presence of noise.

TABLE 2. SNR of the entered signal to the reset line of the reset element for these CgLp controllers.

Signal	C_{R}	$C_{\mathrm{R}'}$	$C_{\mathrm{R}''}$
SNR (dB)	20.26	0.10	1.14

For a deeper insight, in Table 2, the Signal to Noise Ratio (SNR) of these three signals are provided. In this paper, SNR is calculated using

$$SNR = \frac{P_{signal}}{P_{noise}}, \tag{25}$$

where P_{signal} and P_{noise} are power of signal (considering till the fifth harmonic) and noise, respectively. As it can be seen from Table 2, the SNR value in the case of C_{R} is significantly higher than the case of $C_{\mathrm{R}'}$. Although using the shaping filter ($C_{\mathrm{R}''}$) reduces the effect of the noise, it is still far from the case of C_{R} in which the reference frequency dominates the reset instants line.

It can be concluded that C_{R} has the best steady-state performance, $C_{\mathrm{R}'}$ has the best transient response, and $C_{\mathrm{R}''}$ can be considered as a trade-off between C_{R} and $C_{\mathrm{R}'}$. This trade-off can be set by tuning the cut-off frequency of the shaping filter. Increasing the cut-off frequency brings $C_{\mathrm{R}''}$ near to $C_{\mathrm{R}'}$ which means improving the transient response. While reducing the cut-off frequency brings $C_{\mathrm{R}''}$ near to C_{R} which results in improving the steady-state response.

V. CONCLUSION

This paper has proposed a frequency-domain tuning method for CgLp compensators based on the defined pseudo-sensitivities for reset control systems. In this method, a PID.CgLp structure was considered, and its parameters were tuned such that the pseudo-sensitivity was minimized under several loop-shaping and stability constraints. In this method, since CgLp compensators are tuned in the frequency-domain considering the iso-damping constraint, systems are robust against gain variations and time-delay. To show the effectiveness of the proposed approach, the performance of a tuned CgLp compensator was compared with a linear PID controller. The results showed that the proposed method achieved more favorable dynamic performance than the PID controller for the precision motion stage. The tracking performance, the disturbance rejection capability, and the noise rejection capability of the system were improved using the CgLp compensator. In addition, it was practically shown that the water-bed effect is broken for this application. Also, without considering quantization and noise, the super-position law almost holds for the specified reference. Finally, among different sequences, it was demonstrated that the traditional sequence of reset control systems has the best steady-state performance while putting lead filters first has an over-damp response. For future studies, effects of noise and quantization error on the super-position law and tuning and configuration of the shaping filter should be deeply investigated.

REFERENCES

[1] A. A. Dastjerdi, B. M. Vinagre, Y. Chen, and S. H. HosseinNia, "Linear fractional order controllers; a survey in the frequency domain," *Annu. Rev. Control*, vol. 47, pp. 51–70, Jan. 2019.
[2] R. H. Middleton, "Trade-offs in linear control system design," *Automatica*, vol. 27, no. 2, pp. 281–292, Mar. 1991.
[3] R. M. Schmidt, G. Schitter, and A. Rankers, *The Design of High Performance Mechatronics: High-Tech Functionality by Multidisciplinary System Integration*, 2nd ed. Amsterdam, The Netherlands: IOS Press, 2014.
[4] J. van Zundert and T. Oomen, "On inversion-based approaches for feedforward and ILC," *Mechatronics*, vol. 50, pp. 282–291, Apr. 2018.
[5] F. Boeren, T. Oomen, and M. Steinbuch, "Iterative motion feedforward tuning: A data-driven approach based on instrumental variable identification," *Control Eng. Pract.*, vol. 37, pp. 11–19, Apr. 2015.
[6] W. Deng and J. Yao, "Asymptotic tracking control of mechanical servosystems with mismatched uncertainties," *IEEE/ASME Trans. Mechatronics*, early access, Oct. 30, 2020, doi: 10.1109/TMECH.2020.3034923.
[7] W. Deng, J. Yao, and D. Ma, "Time-varying input delay compensation for nonlinear systems with additive disturbance: An output feedback approach," *Int. J. Robust Nonlinear Control*, vol. 28, no. 1, pp. 31–52, Jan. 2018.
[8] J. Hu, Y. Cui, C. Lv, D. Chen, and H. Zhang, "Robust adaptive sliding mode control for discrete singular systems with randomly occurring mixed time-delays under uncertain occurrence probabilities," *Int. J. Syst. Sci.*, vol. 51, no. 6, pp. 987–1006, Apr. 2020.
[9] W. Deng and J. Yao, "Extended-State-Observer-Based adaptive control of electrohydraulic servomechanisms without velocity measurement," *IEEE/ASME Trans. Mechatronics*, vol. 25, no. 3, pp. 1151–1161, Jun. 2020.
[10] I. Horowitz and P. Rosenbaum, "Non-linear design for cost of feedback reduction in systems with large parameter uncertainty," *Int. J. Control*, vol. 21, no. 6, pp. 977–1001, Jun. 1975.
[11] L. Chen, N. Saikumar, and S. H. HosseinNia, "Development of robust fractional-order reset control," *IEEE Trans. Control Syst. Technol.*, vol. 28, no. 4, pp. 1404–1417, Jul. 2020.
[12] Y. Guo, Y. Wang, and L. Xie, "Frequency-domain properties of reset systems with application in Hard-Disk-Drive systems," *IEEE Trans. Control Syst. Technol.*, vol. 17, no. 6, pp. 1446–1453, Nov. 2009.
[13] J. C. Clegg, "A nonlinear integrator for servomechanisms," *Trans. Amer. Inst. Electr. Eng. II, Appl. Ind.*, vol. 77, no. 1, pp. 41–42, 1958.
[14] O. Beker, C. V. Hollot, Y. Chait, and H. Han, "Fundamental properties of reset control systems," *Automatica*, vol. 40, no. 6, pp. 905–915, Jun. 2004.
[15] D. Wu, G. Guo, and Y. Wang, "Reset integral-derivative control for HDD servo systems," *IEEE Trans. Control Syst. Technol.*, vol. 15, no. 1, pp. 161–167, Jan. 2007.
[16] A. Pavlov, B. Hunnekens, N. Wouw, and H. Nijmeijer, "Steady-state performance optimization for nonlinear control systems of Lurâe type," *Automatica*, vol. 49, no. 7, pp. 2087–2097, 2013.
[17] L. Hazeleger, M. Heertjes, and H. Nijmeijer, "Second-order reset elements for stage control design," in *Proc. Amer. Control Conf. (ACC)*, Jul. 2016, pp. 2643–2648.
[18] R. Beerens, A. Bisoffi, L. Zaccarian, W. P. M. H. Heemels, H. Nijmeijer, and N. van de Wouw, "Reset integral control for improved settling of PID-based motion systems with friction," *Automatica*, vol. 107, pp. 483–492, Sep. 2019.
[19] U. Raveendran Nair, R. Costa-Castelló, and A. Baños, "Reset control for DC–DC converters: An experimental application," *IEEE Access*, vol. 7, pp. 128487–128497, 2019.
[20] J. Bernat, J. Kołota, and D. Cieślak, "Reset strategy for output feedback multiple models MRAC applied to DEAP," *IEEE Access*, vol. 8, pp. 120905–120915, 2020.
[21] Z. Gao, Y. Liu, and Z. Wang, "On stabilization of linear switched singular systems via P-D state feedback," *IEEE Access*, vol. 8, pp. 97007–97015, 2020.
[22] Y. Liu, C. Dong, W. Zhang, and Z.-J. Zhou, "Performance-guaranteed switching adaptive control for nonlinear systems with multiple unknown control directions," *IEEE Access*, vol. 8, pp. 35905–35915, 2020.
[23] N. Saikumar, R. K. Sinha, and S. H. HosseinNia, "'Constant in gain lead in phase' Element–application in precision motion control," *IEEE/ASME Trans. Mechatronics*, vol. 24, no. 3, pp. 1176–1185, Jun. 2019.
[24] L. Zaccarian, D. Nesic, and A. R. Teel, "First order reset elements and the Clegg integrator revisited," in *Proc. Amer. Control Conf.*, vol. 1, 2005, pp. 563–568.
[25] Y. Luo, Y. Chen, Y. Pi, C. A. Monje, and B. M. Vinagre, "Optimized fractional order conditional integrator," in *Proc. Amer. Control Conf.*, Jun. 2010, pp. 6686–6691.

[26] A. Barreiro, A. Baños, S. Dormido, and J. A. González-Prieto, "Reset control systems with reset band: Well-posedness, limit cycles and stability analysis," *Syst. Control Lett.*, vol. 63, pp. 1–11, Jan. 2014.
[27] A. Baños and M. A. Davó, "Tuning of reset proportional integral compensators with a variable reset ratio and reset band," *IET Control Theory Appl.*, vol. 8, no. 17, pp. 1949–1962, Nov. 2014.
[28] J. Zheng, Y. Guo, M. Fu, Y. Wang, and L. Xie, "Improved reset control design for a PZT positioning stage," in *Proc. IEEE Int. Conf. Control Appl.*, Oct. 2007, pp. 1272–1277.
[29] A. Baños and A. Barreiro, *Reset Control Systems*. London, U.K.: Springer, 2011.
[30] P. W. J. M. Nuij, M. Steinbuch, and O. H. Bosgra, "Experimental characterization of the stick/sliding transition in a precision mechanical system using the third order sinusoidal input describing function," *Mechatronics*, vol. 18, no. 2, pp. 100–110, Mar. 2008.
[31] S. J. A. M. Van den Eijnden, Y. Knops, and M. F. Heertjes, "A hybrid integrator-gain based low-pass filter for nonlinear motion control," in *Proc. IEEE Conf. Control Technol. Appl. (CCTA)*, Aug. 2018, pp. 1108–1113.
[32] A. Palanikumar, N. Saikumar, and S. H. HosseinNia, "No more differentiator in PID: Development of nonlinear lead for precision mechatronics," in *Proc. Eur. Control Conf. (ECC)*, Jun. 2018, pp. 991–996.
[33] D. Valério, N. Saikumar, A. A. Dastjerdi, N. Karbasizadeh, and S. H. HosseinNia, "Reset control approximates complex order transfer functions," *Nonlinear Dyn.*, vol. 97, pp. 2323–2337, Jul. 2019.
[34] H. Xiaojun, A. Ahmadi Dastjerdi, N. Saikumar, and S. HosseinNia, "Tuning of 'constant in gain Lead in phase (CgLp)' reset controller using higher-order sinusoidal input describing function (HOSIDF)," in *Proc. Austral. New Zealand Control Conf. (ANZCC)*, 2020, pp. 1–6.
[35] M. S. Bahnamiri, N. Karbasizadeh, A. A. Dastjerdi, N. Saikumar, and S. HosseinNia, "Tuning of CgLp based reset controllers: Application in precision positioning systems," in *Proc. Austral. New Zealand Control Conf. (ANZCC)*, 2020, pp. 1–8.
[36] P. W. J. M. Nuij, O. H. Bosgra, and M. Steinbuch, "Higher-order sinusoidal input describing functions for the analysis of non-linear systems with harmonic responses," *Mech. Syst. Signal Process.*, vol. 20, no. 8, pp. 1883–1904, Nov. 2006.
[37] S. Engelberg, "Limitations of the describing function for limit cycle prediction," *IEEE Trans. Autom. Control*, vol. 47, no. 11, pp. 1887–1890, Nov. 2002.
[38] M. Haeringer, M. Merk, and W. Polifke, "Inclusion of higher harmonics in the flame describing function for predicting limit cycles of self-excited combustion instabilities," in *Proc. Combustion Inst.*, 2019, vol. 37, no. 4,'pp. 5255–5262.
[39] K. Heinen, "Frequency analysis of reset systems containing a Clegg integrator," M.S. thesis, Delft Univ. Technol., Delft, The Netherlands, 2018.
[40] A. A. Dastjerdi, A. Astolfi, N. Saikumar, N. Karbasizadeh, D. Valerio, and S. H. HosseinNia, "Closed-loop frequency analysis of reset control systems," Jan. 2020, *arXiv:2001.10487*. [Online]. Available: http://arxiv.org/abs/2001.10487
[41] P. S. V. Nataraj and J. J. Barve, "Reliable and accurate algorithm to compute the limit cycle locus for uncertain nonlinear systems," *IEE Proc.—Control Theory Appl.*, vol. 150, no. 5, pp. 457–466, Sep. 2003.
[42] B. Armstrong-Helouvry and B. Amin, "PID control in the presence of static friction: Exact and describing function analysis," in *Proc. Amer. Control Conf. (ACC)*, vol. 1, 1994, pp. 597–601.
[43] P. Subramanian, V. Gupta, B. Tulsyan, and R. Sujith, "Can describing function technique predict bifurcations in thermoacoustic systems?" in *Proc. 16th AIAA/CEAS Aeroacoust. Conf.*, Jun. 2010, p. 3860.
[44] C. Cai, A. A. Dastjerdi, N. Saikumar, and S. H. HosseinNia, "The optimal sequence for reset controllers," in *Proc. Eur. Control Conf. (ECC)*, May 2020, pp. 1826–1833.
[45] N. Karbasizadeh, A. A. Dastjerdi, N. Saikumar, D. Valerio, and S. H. HosseinNia, "Benefiting from linear behaviour of a nonlinear reset-based element at certain frequencies," in *Proc. Austral. New Zealand Control Conf. (ANZCC)*, Nov. 2020, pp. 1–7.
[46] A. A. Dastjerdi, A. Astolfi, and S. H. HosseinNia, "A frequency-domain stability method for reset systems," in *Proc. 59th IEEE Conf. Decis. Control (CDC)*, Dec. 2020, pp. 5785–5791.
[47] N. Saikumar, D. Valério, and S. H. HosseinNia, "Complex order control for improved loop-shaping in precision positioning," in *Proc. IEEE 58th Conf. Decis. Control (CDC)*, Dec. 2019, pp. 7956–7962.
[48] Y. Guo, L. Xie, and Y. Wang, *Analysis and Design of Reset Control Systems*. London, U.K.: Institution of Engineering and Technology, 2015.
[49] S. Polenkova, J. W. Polderman, and R. Langerak, "Stability of reset systems," in *Proc. 20th Int. Symp. Math. Theory Netw. Syst.*, 2012, pp. 9–13.
[50] P. Vettori, J. W. Polderman, and R. Langerak, "A geometric approach to stability of linear reset systems," in *Proc. 21st Math. Theory Netw. Syst.*, 2014, pp. 776–783.
[51] S. J. A. M. van den Eijnden, M. F. Heertjes, W. P. M. H. Heemels, and H. Nijmeijer, "Hybrid integrator-gain systems: A remedy for overshoot limitations in linear control?" *IEEE Control Syst. Lett.*, vol. 4, no. 4, pp. 1042–1047, Oct. 2020.
[52] J. Sabatier, P. Lanusse, P. Melchior, and A. Oustaloup, *Fractional Order Differentiation and Robust Control Design*, vol. 77. Dordrecht, The Netherlands: Springer, 2015.
[53] E. Grassi and K. Tsakalis, "PID controller tuning by frequency loop-shaping: Application to diffusion furnace temperature control," *IEEE Trans. Control Syst. Technol.*, vol. 8, no. 5, pp. 842–847, Sep. 2000.
[54] R. Nagamune, "Closed-loop shaping based on Nevanlinna–pick interpolation with a degree bound," *IEEE Trans. Autom. Control*, vol. 49, no. 2, pp. 300–305, Feb. 2004.
[55] X. Chen, T. Jiang, and M. Tomizuka, "Pseudo Youla–Kucera parameterization with control of the waterbed effect for local loop shaping," *Automatica*, vol. 62, pp. 177–183, Dec. 2015.
[56] T. Jiang, H. Xiao, J. Tang, L. Sun, and X. Chen, "Local loop shaping for rejecting band-limited disturbances in nonminimum-phase systems with application to laser beam steering for additive manufacturing," *IEEE Trans. Control Syst. Technol.*, vol. 28, no. 6, pp. 2249–2262, Nov. 2020.
[57] J. M. Díaz, R. Costa-Castelló, R. Muñoz, and S. Dormido, "An interactive and comprehensive software tool to promote active learning in the loop shaping control system design," *IEEE Access*, vol. 5, pp. 10533–10546, 2017.
[58] B. Mohandes, I. Boiko, and Y. Abdel-Magid, "Control system loop-shaping as a mathematical optimization problem: An ensemble of models," *IEEE Access*, vol. 8, pp. 137185–137197, 2020.
[59] W. Guan, W. Cao, J. Sun, and Z. Su, "Steering controller design for smart autonomous surface vessel based on CSF L_2 gain robust strategy," *IEEE Access*, vol. 7, pp. 109982–109989, 2019.
[60] S. Al-Amer and F. Al-Sunni, "Approximation of time-delay systems," in *Proc. Amer. Control Conf. (ACC)*, vol. 4, Jun. 2000, pp. 2491–2495.
[61] A. A. Dastjerdi. *Toolbox for Frequency Analysis of Reset Control Systems*. Accessed: Jun. 2020. [Online]. Available: https://www.tudelft.nl/en/3me/about/departments/precision-and-microsystems-engineering-pme/research/mechatronic-system-design-msd/msd-research/motion-control/toolbox-frequency-analysis-of-reset-control-systems/
[62] A. A. Dastjerdi, N. Saikumar, and S. H. HosseinNia, "Tuning guidelines for fractional order PID controllers: Rules of thumb," *Mechatronics*, vol. 56, pp. 26–36, Dec. 2018.
[63] B. Kieft, "Proposed solutions for quantization induced performance deterioration in reset controllers," M.Sc. dissertation, Delft Univ. Technol., Delft, The Netherlands, 2020.
[64] A. A. Dastjerdi, A. Astolfi, and S. H. HosseinNia, "Frequency domain stability method for reset systems," 2020, *arXiv:2009.00569*. [Online]. Available: http://arxiv.org/abs/2009.00569

ALI AHMADI DASTJERDI (Member, IEEE) received the master's degree in mechanical engineering from the Sharif University of Technology, Iran, in 2015. He is currently pursuing the Ph.D. degree with the Department of Precision and Microsystem Engineering, TU Delft, The Netherlands. His primary research interests include mechatronic systems design, precision engineering, precision motion control, and nonlinear control.

S. HASSAN HOSSEINNIA (Senior Member, IEEE) received the Ph.D. degree (Hons.) *(cum laude)* in electrical engineering specializing in automatic control: application in mechatronics, form the University of Extremadura, Spain, in 2013. His main research interests include precision mechatronic system design, precision motion control, and mechatronic system with distributed actuation and sensing. He has an industrial background working at ABB, Sweden. Since October 2014, he has been appointed as an Assistant Professor with the Department of Precession and Microsystem Engineering, TU Delft, The Netherlands. He is currently an Associate Editor of the *International Journal of Advanced Robotic Systems* and *Journal of Mathematical Problems in Engineering*.